SEA and Local Energy Approach of fluid-filled pipes

A. Bocquillet, M. N. Ichchou, A. LeBot and L. Jezequel
Laboratoire Tribologie et de Dynamique des Systèmes, Ecole Centrale de Lyon,
36 Av Guy de Collongue, 69130 Ecully Cedex, FRANCE

Abstract

Prediction of averaged vibrational response of coupled fluid-structure systems is dealt with in this paper. The focus is the Donnell-Mushtari cylindrical shell with an internal acoustic fluid, a typical example of waveguides with multiple transmission mechanisms. "Exact" and statistical approaches are developped for this system. A state vector approach is first proposed; it allows the characterization of propagating modes from a general manner. This propagating content leads to the formulation of the **L***ocal* **E***nergy* **A***pproach as well as the* **SEA** *for this canonical problem.*

1 Introduction

The high frequency behaviour of complex structures is a subject of increasing research and interest. Deterministic approaches reveals inadaquate in high frequency range and from a statistical point of view : Uncertainty exists in the geometric or material properties of the mechanical systems. Among alternatives proposed for the frequency analysis, the well known **SEA** [1] as well as the **L**ocal **E**nergy **A**pproach [2,3] are considered in this paper.

The proposed work investigates the energy aspects of a canonical fluid-structure problem, more particularly fluid-filled pipes. Up to now, the high frequency analysis of such structures by means of S.E.A or alternatives remains an important issue and a susbject of research and developments, due to the intrinsic dynamics involving fluid structure coupling effects.

From a state space formulation of the problem, the propagating behaviour of such systems is easily obtained. The propagating content when used according to a number of assumptions discussed in the paper leads to a relevant representation of energy exchanges between propagating modes and to the energy spread within "subsystems". On the one hand, an SEA model is identified according to the propagating contents. On the other hand, the same inputs allow a **L**ocal **E**nergy **A**pproach to be written. Comparative results are given in order to show the robustness of the proposed methodology.

2 Formulation of the propagating approach for an elastoacoustic problem

The problem, which is considered here is a basic elastoacoustic problem (Figure 1). It consists in a cylindrical shell with an internal acoustic fluid. The shell obeys the Donnell-Mushtari theory [10], and the linearized Helmholtz equation characterizes fluid behaviour. In the following subsections, a state space formulation is summarized and the propagation for the elasto-acoustic

problem is discussed.

2.1 Structural shell Dynamics

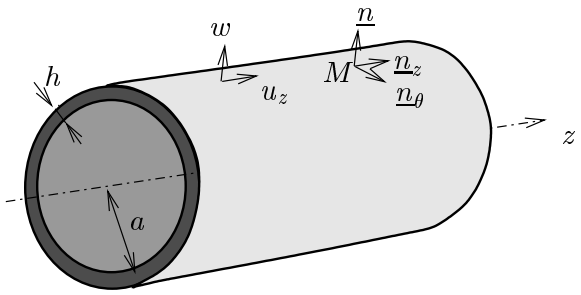

FIG. 1: *A Donnell-Mushtari cylindrical shell.*

h, a respectively designate the thickness and the radius of the studied cylindrical shell. E, ν and ρ will respectively denote the Young modulus, Poisson coefficient and the mass density of the material. u_z, w represent the axial and the bending motion of the shell. ϕ will be associated to the bending motion w. The normal, transverse forces as well as bending moments are respectively N_z, T and M_z. For the axisymetric dynamics, the functional associated to the undamped Donnel-Mushtari cylindrical shell theory can be found to be:

$$\mathcal{F}^{(s)} = \frac{2\,\pi a}{4}\int_z (D\frac{d\phi}{d\,z}\frac{d\,\phi^*}{d\,z} + C\,(\frac{d\,u_z}{d\,z} + \nu\frac{w}{a})\frac{d\,u_z}{d\,z}^* + C\,(\nu\,\frac{d\,u_z}{d\,z} + \frac{w}{a})\frac{w}{a}^* - \rho\,h\,\omega^2(u_z\,u_z^* + w\,w^*) + T^*(\phi - \frac{d\,w}{dz}) + T(\phi^* - \frac{d\,w}{dz}^*))\,dz.$$

where $C = \frac{Eh}{1-\nu^2}$ and $D = \frac{Eh^3}{12(1-\nu^2)}$. The time dependancy of motion is assumed to be $e^{i\omega t}$. The upperscript s in all what follows designates variables linked to the structure. Let's define $u^{(s)}$ and $f^{(s)}$ by:

$$\underline{u}^{(s)} = \begin{pmatrix} u_z \\ w \\ \phi \end{pmatrix} \quad \text{et } \underline{f}^{(s)} = \begin{pmatrix} N_z \\ -T \\ M_z \end{pmatrix} \tag{1}$$

The equation of motions can thus be formulated from the functional as [2]:

$$\underline{\underline{J_a}}^{(s)}\frac{d}{d\,z}\begin{pmatrix}\underline{u}^{(s)} \\ \underline{f}^{(s)}\end{pmatrix} = \underline{\underline{H}}^{(s)}\begin{pmatrix}\underline{u}^{(s)} \\ \underline{f}^{(s)}\end{pmatrix} \tag{2}$$

where:

$$\underline{\underline{H}}^{(s)} = \begin{pmatrix} \rho h\omega^2 & 0 & 0 & 0 & 0 & 0 \\ 0 & \frac{h(-E+\rho\omega^2a^2)}{a^2} & 0 & -\frac{\nu}{a} & 0 & 0 \\ 0 & 0 & 0 & 0 & 1 & 0 \\ 0 & -\frac{\nu}{a} & 0 & \frac{1}{C} & 0 & 0 \\ 0 & 0 & 1 & 0 & 0 & 0 \\ 0 & 0 & 0 & 0 & 0 & \frac{1}{D} \end{pmatrix}. \tag{3}$$

$\underline{\underline{J_a}}^{(s)}$ is a simplectic 6×6 matrix and $\underline{\underline{H}}^{(s)}$ is found to be symmetrical. This symmetry establishes the mathematical properties of the the state-space equation [8]. The latter appears to be a simple presentation of the equation of motion, and it can be compared to the expressions given by Wang [5].

2.2 Fluid-structure functional

The bounded internal acoustic fluid inside the pipe (volume Ω) is governed by the linear Helmoltz equation. Considering $\partial\Omega$ as being the internal boundary of the bounded fluid and denoting $\mathbf{n}$ its unit normal, it comes:

$$\begin{array}{ll} \Delta \mathrm{p} + \mathbf{k^2}\,\mathrm{p} = 0 & \text{in}\,\Omega \quad (a) \\ \frac{\partial \mathrm{p}}{\partial n} = \rho_f \omega^2\, w & \text{on}\,\partial\Omega. \quad (b) \end{array} \tag{4}$$

with $\mathbf{k} = \omega/c$ real valued. The functional associated to the first equation and the coupling between the two media, namely equation (4) are introducted by:

$$\mathcal{F}^{(a)} = \frac{1}{4}\int_{\Omega} ({}^t(\underline{\underline{\nabla}}\mathrm{p}^*)(\underline{\underline{\nabla}}\mathrm{p}) - \mathbf{k}^2\mathrm{p}^*\mathrm{p})\, dV, \quad \mathcal{F}^{(s,a)} = -\frac{1}{2}\int_{\partial\Omega} {}^t(\underline{w}^*\mathrm{p} + \underline{w}\mathrm{p}^*) dS \tag{5}$$

Finally, the functional of the coupled fluid structure problem considered here can be summarized as follows:

$$\mathcal{F} = \mathcal{F}^{(a)} + \mathcal{F}^{(s)} + \mathcal{F}^{(s,a)} \tag{6}$$

The state space formulation for the coupled fluid structure problem needs to be considered now. It will be achieved by using a particular approximation of the acoustic field.

2.3 propagating approach formulation

In the high frequency range, the non-planar dynamics in the fluid has to be taken into account. The acoustic pressure field $\mathrm{p}(r,\theta,z)$ is approximated using suitable decomposition functions. A separation of variables is proposed by Finnveden [9], who used a finite element discretisation with polynomials of high degree for the fluid section. Here we propose the decomposition of pressure on bessel functions : for the axi-symetric motion, an appropriate approximation of the acoustic internal field can be shown to [11]

$$\mathrm{p}(r,\theta,z) = \sum_{j=1}^{n} \frac{J_0(\vartheta_j\,\frac{r}{a})}{\sqrt{\pi} J_0(\vartheta_j)} p_j(z). \tag{7}$$

where ϑ_j designate the jth root of the Bessel function of the first kind. It should be noted that the orthogonal Bessel function properties secure convergence of the given approximation. Using the given decomposition with combination of the coupled functional of the problem (6), one can readily obtain the following state space formulation for the coupled elastoacoustic problem:

$$\underline{\underline{J_a}}^{(c)} \frac{d\underline{Y}^{(c)}}{dz} = \underline{\underline{H}}^{(c)} \underline{Y}^{(c)} \tag{8}$$

where the state space vector and matrix $\underline{\underline{H}}^{(c)}$ are [2]:

$$\underline{Y}^{(c)} = \begin{pmatrix} \underline{p} \\ \underline{u} \\ w \\ \phi \\ \underline{f}^{(a)} = \frac{1}{\rho_f \omega^2}\underline{\underline{M}}^{(a)} \frac{d\underline{p}}{dz} \\ 2\,\pi\, a\, N_z \\ -2\,\pi\, a\, T \\ 2\,\pi\, a\, M_z \end{pmatrix}, \qquad \underline{\underline{H}}^{(c)} = \begin{pmatrix} \frac{1}{\rho\omega^2}\underline{\underline{K}}^{(a)} & {}^t\underline{\underline{B}} & 0 & 0 \\ \underline{\underline{B}} & \underline{\underline{K}}^{(s)} & 0 & \underline{\underline{Q}}^{(s)} \\ 0 & 0 & \rho\omega^2\underline{\underline{M}}^{(a)} & 0 \\ 0 & {}^t\underline{\underline{Q}}^{(s)} & 0 & \underline{\underline{M}}^{(s)} \end{pmatrix}. \tag{9}$$

The expressions of $\underline{\underline{J_a}}^{(c)}$, $\underline{\underline{B}}$, $\underline{\underline{M}}^{(s)}$, $\underline{\underline{K}}^{(s)}$, $\underline{\underline{Q}}^{(s)}$ are added in Appendix. The matrices $\underline{\underline{M}}^{(a)}$ and $\underline{\underline{K}}^{(a)}$ are diagonal such that:

$$M^{(a)}_{j,j} = \frac{1}{a^2};\ K^{(a)}_{j,j} = (a^2 * \mathbf{k}^2 - \vartheta_j^2); \tag{10}$$

The state space formulation for the coupled elastoacoustic problem is now established. Fundamental solutions of (8) are exponential dependent. The generalized eigenvalue form, of the following expression

$$-i\,k_j \underline{\underline{J_a}}^{(c)} \underline{V}^{(c)}_j = \underline{\underline{H}}^{(c)} \underline{V}^{(c)}_j, \tag{11}$$

provides the wavenumbers k_j and associated propagation modes $\underline{V}^{(c)}_j$. This determination of propagation is a numerical alternative to non-linear approaches used by Fuller [6]. The propagation for dissipative waveguides is also possible. In this case $\underline{\underline{H}}^{(c)}$ becomes complex symmetrical.

2.4 Results and comments

Dispersion curves are given in the case of a steel shell filled with water. The mechanical/geometrical characteristics of the system are summarized in Table 1.

	h/a	ρ	ρ_f	c	E	ν	η
shell	.05	$7800Kg/m^3$	-	-	$19.2e10N/m^2$	.3	0.01
water	-	-	$1000Kg/m^3$	1500 m/s	-	-	-

TAB. 1: *table of characteristics*

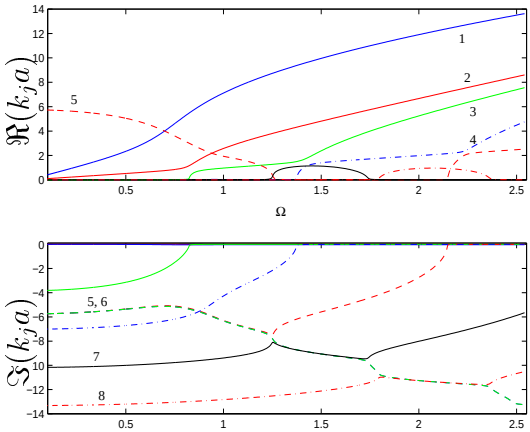

FIG. 2: *Dispersion curve for the Donnell-Mushtari cylindrical shell coupled with an internal fluid.*

Ω is the non dimensional frequency $\Omega = \omega\, a/c_s$, where $c_s = \sqrt{e/\rho_s/(1-\nu^2)}$ corresponds to the extensional phase speed of the shell material. It should be adressed that convergence is reached with a small number of approximation functions for the pressure field. Figure 2 gives the real and imaginary parts of the wavenumbers extracted from the state space formulation obtained in the damped case. For the comment of the dispersion curves, we can refer to Fuller [6]. In the low frequency range, the first branch corresponds to a fluid mode. When frequency increases,

coupling effects takes place, involving radial displacement. At the beginning, the second branch is essentially a dilatational mode. Around the ring frequency ($\Omega = 1$), the pressure in the fluid becomes close to the release dilational mode. In the frequency interval $\Omega \in [0, 2.5]$, up to 5 modes can propagate far from the discontinuities in each direction.

3 Local Energy Approach formulation

In this section, the **L**ocal **E**nergy **A**pproach as well as the **SEA** for the canonical problem considered in this paper will be derived. The latter will be extracted from the global energy balance given by the **LEA**.

3.1 Basic Energy formulas from the propagating approach

The propagating approach exposed in the previous section provides a set of J-orthogonal propagation modes [8]. They form a new basis for the dynamical motion of the elastoacoustic problem. In fact, the state vector can be expressed as the linear superposition of the given propagation modes :

$$\underline{Y}^{(c)}(z) = \underline{\underline{V}}\,\underline{\mu}(z) \tag{12}$$

$\underline{\underline{V}}$ being the matrix of $2n$ propagating modes computed from equation (11). Indeed, the computation of the kinematic solution can be provided using the change of variables (12) and a set of suitable boundary conditions. In the context of this paper, the problem represented in Figure 3 will be considered in depth.

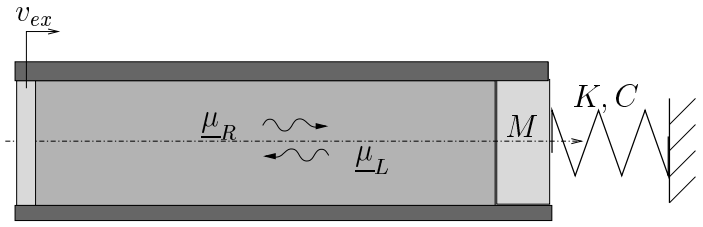

FIG. 3: *Pipe excited on z=0 with a mass/spring-damper system on z=L.*

The acoustic boundary conditions written in terms of the state vector components are as follows:

$$\begin{array}{l} f_j^{(a)}(0) = -\frac{i\sqrt{(pi)a^2}}{\omega} v_{ex}\,\delta_1(j) \\ f_j^{(a)}(L) = -\frac{\pi\sqrt{(pi)a^4}}{K_d}\,p_1(L)\delta_1(j) \\ \text{with } K_d = -M\,\omega^2 + iC\omega + K \end{array} \tag{13}$$

The propagating vector $\underline{\mu}(z)$ can be separated into right-propagating wave vector $\underline{\mu}_R$ and left-propagating wave vector designated by $\underline{\mu}_L$. The boundary conditions can be written in terms of waves as follows:

$$\underline{\mu}_R(0) = \underline{\underline{C}}^{(1)}\underline{\mu}_L(0) + \underline{\mu}_{ex}, \qquad \underline{\mu}_L(L) = \underline{\underline{C}}^{(2)}\underline{\mu}_L(L) \tag{14}$$

where $\underline{\mu}_{ex}$ is the incident wave associated to the imposed speed at $z = 0$. The expression (14) corresponds to the reflections of both ends, where $\underline{\underline{C}}^{(1)}$ and $\underline{\underline{C}}^{(2)}$ are the generalized reflection matrices. To complete the wave analysis of the given problem, the wave transport phenomenon must be introduced. The relation between the wave vector at any section and the boundaries is thus given by [14]:

$$\underline{\mu}(z) = \begin{pmatrix} \underline{\underline{D}}(z) & 0 \\ 0 & \underline{\underline{D}}(L-z) \end{pmatrix} \begin{pmatrix} \underline{\mu}_R(0) \\ \underline{\mu}_L(L) \end{pmatrix} \quad \text{with} \quad \underline{\underline{D}}(z) = \underline{\underline{diag}}(e^{-ik_j z}) \tag{15}$$

Expressions (14,15) provide the solution system of the elastoacoustic problem in terms of wave vectors $\underline{\mu}$. Reconstruction of the state vector solution is then readily obtained using expression (12). Expression of power flow $\Pi(z)$ in the elastoacoustic waveguide can thus be computed as follows [2,15]:

$$\Pi(z) = -\frac{i\,\omega}{4}\, {}^t\underline{Y}^{(c)*}(z)\underline{\underline{J_a}}\underline{Y}^{(c)}(z) = {}^t\underline{\mu}^*(z)\,\underline{\underline{P}}\,\underline{\mu}(z) \tag{16}$$

with:

$$\underline{\underline{P}} = -\frac{i\,\omega}{4}\, {}^t\underline{\underline{V}}^*\,\underline{\underline{J_a}}\,\underline{\underline{V}} \tag{17}$$

In the case of dissipative waveguide, the power matrix $\underline{\underline{P}}$ is full. So out-of-diagonal terms contribute to the power flow at any section of the pipe. The computation of energy densities (kinetic and potential) can also be done in a similar manner.

3.2 Energy balance at boundaries

From a partition of $\underline{\mu}$ into incident waves ($\underline{\mu}_I$) and scattered waves ($\underline{\mu}_S$) one can easily define the incident and reflected powers at the boundary $z = L$ using the following bilinear forms:

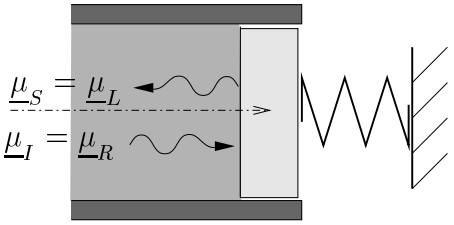

FIG. 4: *Scattering of propagation modes μ_{R_j} on the boundary* (2).

$$\begin{aligned} \Pi_I(L) &= {}^t\,\underline{\mu}(L)^*\underline{\underline{P}}_I\underline{\mu}(L), \\ \Pi_S(L) &= {}^t\,\underline{\mu}(L)^*\underline{\underline{P}}_S\underline{\mu}(L). \end{aligned} \tag{18}$$

The following definition for power matrices insures that the reflected power is smaller than incident power :

$$\underline{\underline{P}}_I = \begin{pmatrix} \underline{\underline{P}}_R & \underline{\underline{P}}_{R,L} \\ \underline{\underline{P}}_{L,R} & 0 \end{pmatrix}, \qquad \underline{\underline{P}}_S = \begin{pmatrix} 0 & 0 \\ 0 & -\underline{\underline{P}}_L \end{pmatrix}. \tag{19}$$

Phase fluctuations of the waves μ_j can be related to variations of frequency, uncertainties on length of the guide, the Young Modulus... Owing to relation (15) the difference of phase between two different propagating waves varies far from discontinuities. Between two incident waves on one singularity, the propagation from the opposite boundary insures that their interference contribution $P_{i,j}\mu^*_{I_i}(L)\mu_{I_j}(L)$ to power flow balances can be neglected. Incident waves are thus assumed to be uncorrelated in what follows. In addition, the reflection coefficients do not always induce enough phase fluctuations, so that interferences between incident and reflected wave and between reflected waves cannot be neglected in any averaged power flow balances. Uncorrelation can be interpreted by a statistical model with the following esperancy hypothesis $\mathcal{E}(\mu^*_{I_i}(L)\mu_{I_j}(L)) = \delta_{ij}\mathcal{E}(|\mu_{I_i}(L)|^2)$, where $\mathcal{E}$ designates the expected value[2]. New parameters denoted σ_{I_i} are thus introduced for the **LEA** derivation to represent $\mathcal{E}(|\mu_{I_i}(L)|^2)$. In this model, the incident power $< \Pi_I >$ can therefore be written as :

$$< \Pi_I(L) >= \sum_{i=1}^{n} P_{i,i}\, \sigma_{I_i}(L). \tag{20}$$

For a unique incident wave μ_{I_i} at the boundary, the exact ratio between incident and reflected power is supposed to be verified by the **LEA**, so that :

$$\frac{< \Pi_S >}{< \Pi_I >} = \frac{\Pi_S}{\Pi_I} = \frac{Pc_{S_{i,i}}}{Pc_{I_{i,i}}}. \tag{21}$$

where $Pc_{I_{i,i}}$ and $Pc_{S_{i,i}}$ are the matrix coefficients of the incident and reflected power after condensation on the incident waves, precisely :

$$\underline{\underline{Pc}}_I = {}^t\left(\underline{\underline{\frac{I}{C^{(2)}}}}\right)^* \underline{\underline{P}}_I \left(\underline{\underline{\frac{I}{C^{(2)}}}}\right); \quad \underline{\underline{Pc}}_S = {}^t\left(\underline{\underline{\frac{I}{C^{(2)}}}}\right)^* \underline{\underline{P}}_S \left(\underline{\underline{\frac{I}{C^{(2)}}}}\right). \tag{22}$$

The reflected power can be thus expressed using the **LEA** incident waves $\sigma_{I_i}(L)$ as follows:

$$< \Pi_S > \overset{H}{=} \sum_{i=1}^{n} \frac{Pc_{S_{i,i}}}{Pc_{I_{i,i}}} P_{i,i}\, \sigma_{I_i}(L). \tag{23}$$

The reflected waves $\underline{\mu}_S = \underline{C}_{.,i}\mu_{I_i}$ tend to uncorrelate themselves away from the singularity. One can asymptotically establish that $\forall z \neq L$ the mean value of reflected power, initially expressed in terms of reflected waves can be derived under the following form :

$$\begin{aligned} \mathcal{E}(\Pi_S^{(2)}(z)) &= -\sum_{j=1}^{n} P_{n1+j,n1+j}\mathcal{E}(|\mu_{S_j}(z)|)^2 \\ &= -[\sum_{j=1}^{n} P_{n1+j,n1+j}|C^2_{j,i}\lambda(L-z)|^2]\,\mathcal{E}(|\mu_{R_i}(L)|^2) \\ &\approx -[\sum_{j=1}^{n} P_{n1+j,n1+j}|C^{(2)}_{j,i}|^2]\;\mathcal{E}(|\mu_{I_i}(L)|^2) \end{aligned} \tag{24}$$

This expression (24) specifies the distribution of reflected power on the reflected waves for the **LEA**. New parameters denoted σ_{S_j} are associated to reflected waves $\mathcal{E}(|\mu_{S_j}|)^2$. The reflected power $< \Pi_S >$ is sought under the following form :

$$< \Pi_S(L) >= -\sum_{i=1}^{n} P_{n+i,n+i}\, \sigma_{S_i}(L) \tag{25}$$

Eventually, an intrinsic relationship linking the incident and the reflected waves σ_{I_i} and σ_{S_i} has to be written. This is done by introducing the efficiency matrix $\underline{\underline{E}}$ so that :

$$\underline{\sigma}_S(L) = \underline{\underline{E}}^{(2)}\,\underline{\sigma}_I(L) \;\text{ with }\quad E^{(2)}_{i,j} = \frac{|C^{(2)}_{i,j}|^2}{\sum\limits_q P_{n1+q,n1+q}|C^{(2)}_{q,j}|^2}\,\frac{Pc_{S_{j,j}}}{Pc_{I_{j,j}}}P_{I_{j,j}}. \tag{26}$$

The first ratio in $E^{(2)}_{i,j}$ specifies the partition of reflected power on the reflected waves. With the second ratio, the **LEA** model verifies the power balance for any incident wave. This definition of efficiency matrix insures that at conservative discontinuities the power flow vanishes. In the case of non-conservative boundaries, the intended sign of power flow will be respected. For the boundary $z = 0$, a similar relation can be found, with the adjonction of a excitation term $\underline{\sigma}_{ex}$:

$$\underline{\sigma}_R(0) = \underline{\underline{E}}^{(1)}\,\underline{\sigma}_L(0) + \underline{\sigma}_{ex} \tag{27}$$

This expression comes from the uncorrelation assumptions. The injected power $\Pi_{inj} = \Pi(0)$ can be parted in five terms

$$\Pi_{inj} = \Pi_{inf} + \Pi_I(0) - \Pi_S(0) + \Pi_{ex,I}(0) + \Pi_{ex,S}(0).$$

Π_{inf} denotes the injected power when the duct is semi-infinite. The terms $\Pi_I(0)$and $\Pi_S(0)$ represent the incident and reflected power flow due to the incident waves coming from the opposite boundary. $\Pi_{ex,I}$, $\Pi_{ex,S}$ are the contribution of interferences between excitation and incident- reflected waves. As the excitation can be viewed as a source of waves, decorrelated from the incident waves μ_{L_j}, the hypothesis $\mathcal{E}(\mu^*_{L_i}(0)\mu_{ex_j}) = 0$ can be used. As this singularity is conservative, the **LEA** power balance on the first boundary may be written as

$$< \Pi_{inj} >= \Pi_{inf} + < \Pi_I(0) > - < \Pi_S(0) >= \Pi_{inf}$$

In this case, the injected power is the one of the semi-infinite pipe. Also, the source contributes in an independant manner to power flow going out of the singularity. As the propagation tends to uncorrelate the waves, the injected power flow can be asymptoticaly distributed on the out-going waves :

$$P_{i,i}\sigma_{ex_i} = \frac{P_{i,i}|\mu_{ex_i}|^2}{\sum\limits_q P_{S_{q,q}}|\mu_{ex_q}|^2}\Pi_{inf} = P_{i,i}r_{ex_i}\Pi_{inf} \tag{28}$$

A more detailed discussion on the subject of power flow balances and uncorrelation can be found in reference [2].

3.3 Energy balance far from singularities

The wave guide can be analyzed using a similar way : it can be viewed as a junction between sections $S(0)$ and $S(L)$. In the two propagation vectors $\underline{\mu}(0)$, $\underline{\mu}(L)$, one can distinguish incident and reflected waves on the guide, as shown in Figure (5).

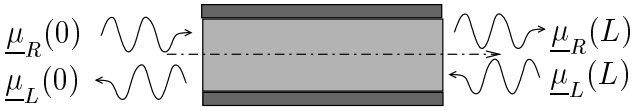

FIG. 5: *Wave transport between two singularities.*

It can be easily shown by using similar power balances and uncorrelation hypothesis as used before, that:

$$\underline{\sigma}(L) = \underline{\underline{D}}(L)\underline{\underline{D}}(L)^* \, \underline{\sigma}(0). \tag{29}$$

The system of resolution on $\underline{\sigma}$ can be constructed with equations (26), (27) and (29). It may be written as

$$\underline{\underline{S}} \begin{pmatrix} \underline{\sigma}(0) \\ \underline{\sigma}(L) \end{pmatrix} = \begin{pmatrix} \underline{\sigma}_{ex} \\ \underline{0} \end{pmatrix} \tag{30}$$

The reconstruction of power flow at any section of the wave-guide is through-out. The bilinear forms of the kinetic and potential energy on the sections can be determined by using the matrices of the differential system. For example, the potential energy is calculated by :

$$Ep(z) =^t \underline{\mu}^*(z)\underline{\underline{K_\mu}}\underline{\mu}(z) \tag{31}$$

Away from boundaries, the simplified model will give smooth energy levels with the following expression

$$\begin{aligned} < Ep(z) >= \sum_{j=1}^{2n} K_{\mu_{j,j}} \sigma_j(z) =^t \underline{K_\mu}^{(d)} \, \underline{\sigma}(z) \\ < Ec(z) >= \sum_{j=1}^{2n} M_{\mu_{j,j}} \sigma_j(z) =^t \underline{M_\mu}^{(d)} \, \underline{\sigma}(z) \end{aligned} \tag{32}$$

Hencefore, determination of the **LEA** unknowns leads to the reconstruction of the energy parameters far from singularities.

3.4 Results and comments

The example proposed before is considered here. Table 1 summarizes the parameters used. The absorber characteristics are as follows: The mass of the piston, the dissipation and the non dimensional natural frequency are respectively $M = \pi a^2 L/100, \xi = 0.05, \Omega_m = 0.28$. A first computation involving the propagating modes was first performed. It allowed calculation of energy density and energy flow without any simplification. This computation provides a reference results for the **LEA** validations. Using the developments given below, the **LEA** model of the fluid-filled pipe was performed.

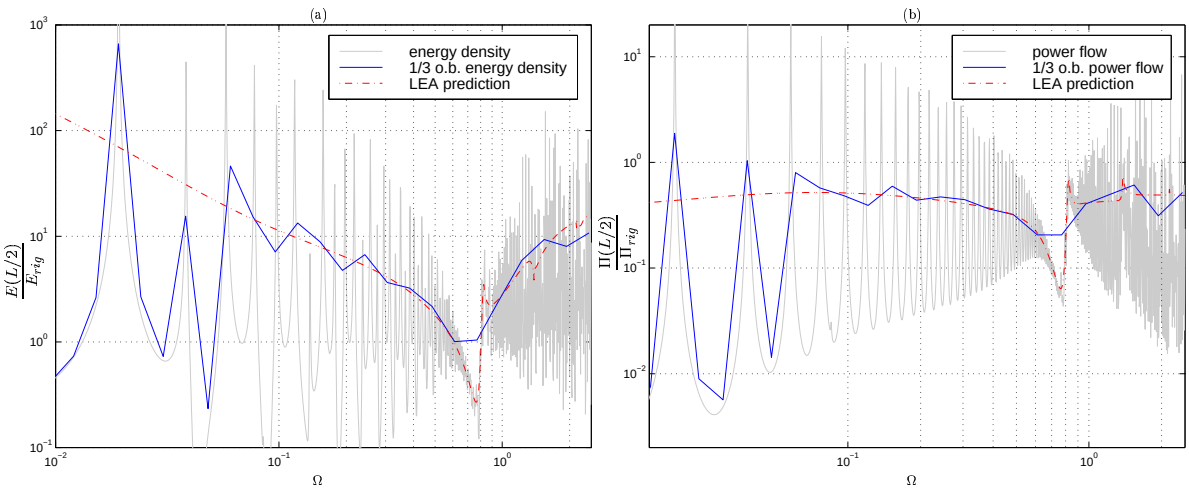

FIG. 6: *Comparison between* ***LEA*** *and exact calculation. Energy (a) and power flow (b) on the section $z = L/2$ of the pipe.*

Figure 6 gives a comparison between both computations on the section located at the middle of the pipe. Ratio of the energy levels to the one of a rigid semi-infinite pipe are plotted. This figure includes a 1/3 octave calculation of the exact energy levels and shows a good agreement with the **LEA** prediction. Stiff variations are observed at cut-on frequencies of propagating modes (3) and (4). In addition, around $\Omega = 0.8$, the two first propagating modes change of nature [6], involving frequency variations in the repartition of energy between propagating modes.

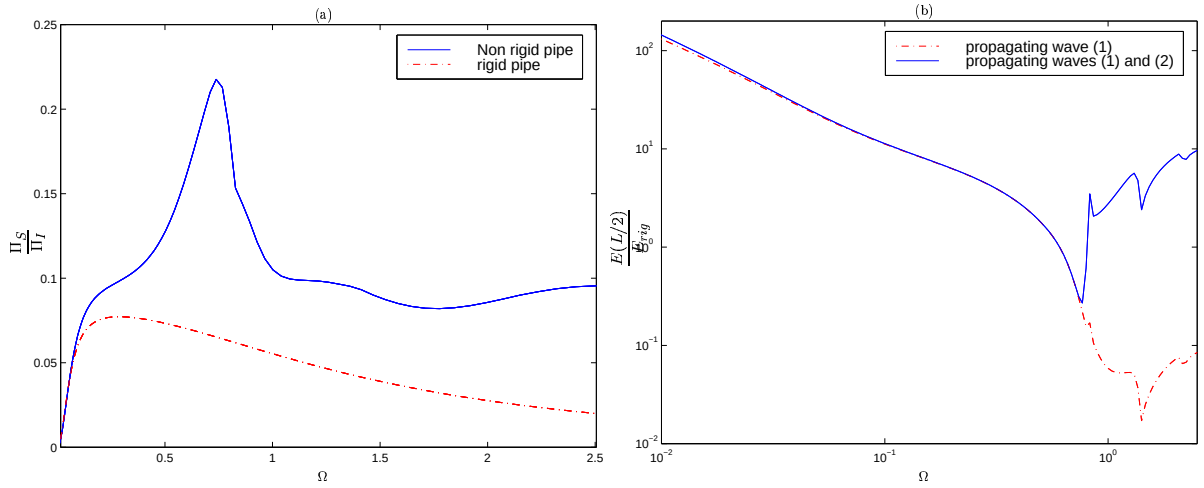

FIG. 7: *(a): Reflection efficiency of boundary z=L. rigid and non rigid pipes. (b): Contribution of wave (1) and waves (1,2) to total energy on section $z = L/2$ for the **LEA** model.*

In Figure 7(a) is represented the energy transmission of the wave (1) to the piston/spring-damper system, for the studied and rigid pipe cases. In the case of the rigid pipe, the maximum of absorbed power corresponds to the natural frequency of the terminaison system; the fluid structure coupling notably modifies the interaction between the first wave and the 1ddl system when the frequency increases. The second result presented in Figure 7(b) considers the propagating complexity role within the context of **LEA** computation. In this figure, the **LEA** results can be compared when several propagating modes are successively taken into account. In low frequencies, the propagating mode (1), which is very close to the plane acoustical wave, contribute in majority to the dynamics of the pipe, as it is easily excited at the boundary $z = 0$. Over $\Omega = 0.8$, this wave changes of nature (the energy is predominant in the structure), and the second wave, becoming a "fluid wave", holds the majority of energy in the section.*It clearly shows, that very poor predictions are obtained when a single propagating mode* **LEA** *computation is proceeded. This result confirms the interest of the proposed propagating approach, in view of high frequency modelling of dynamics.*

4 SEA considerations for the elastoacoustic problem

With the previous developments, a relation between the vector $\underline{\sigma}$ at one section and the injected power is straightforward : using relationships (30) and $\underline{\sigma}(z) = \underline{\underline{D}}(z)\underline{\underline{D}}(z)^* \, \underline{\sigma}(0)$, we have

$$\underline{\sigma}(z) = \underline{\underline{Q}}(z)\underline{r}_{ex} \quad < \Pi_{inj} > .$$

With the propagating approach, The potential energy of the duct can also be related to the injected power. The obtained levels are smooth and are based on underlying uncorrelation

assumptions :

$$\eta_c\,\omega\ <E>=<\Pi_{inj}>$$
$$with$$
$$(\eta_c\,\omega)^{-1} =^t (\underline{K_\mu}^{(d)} + \underline{M_\mu}^{(d)}) \int_{z=0}^{L} \underline{\underline{Q}}(z)\,dz\,\underline{r}_{ex}$$

In this expression, no hypothesis is made on the nature of the excitation which is located at one end of the guide. The approach, developed on a single system in this paper, can be applied to coupled systems and can give the global matrix of coupling loss factors.

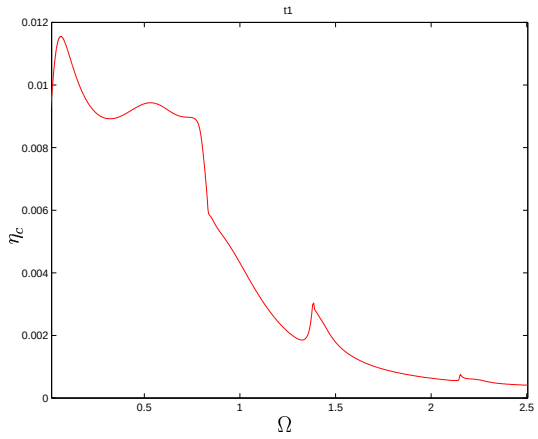

FIG. 8: *SEA parameter η_c of the pipe-1ddl system*

In Figure 8, the drastic variations of the damping loss factor correspond to cut-on frequencies. The dissipation effect is more important in the lower frequency range, when the first propagating mode, which strongly interacts with the right boundary, is predominant.

5 Concluding remarks

In this paper, formulation and generalization of a propagating approach to elastoacoustic problems have been presented. The propagation approach provides a relevant description to the statistical analysis of power transfer. The propagating modes are used as a set of input data in view of the definition of the **L**ocal **E**nergy **A**pproach as well as the **SEA**. The fluid-filled pipe system given in this paper is an illustration of the general procedure developed for complex waveguide networks.

6. Acknowledgments.

Part of the research presented here is based on a contract with Electricity of France. The authors gratefully acknowledge Mr E. Luzzato (EDF/DER, Paris) for his support.

7. References.

[1] R.H. Lyon, *Statistical Energy Analysis of Dynamical Systems: Theory and Application*, (Cambridge, Massachusetts, MIT Press, 1975).
[2] A. Bocquillet, Thèse à l'Ecole Centrale de Lyon, 00-ECDL-01, *Méthodes énergétiques de caractérisations vibroacoustiques des réseaux complexes*, (2000).

[3] M.N. Ichchou, Thèse à l'Ecole Centrale de Lyon, 96-ECDL-10, *Formulations énergétiques pour l'étude moyennes et hautes fréquences des systèmes* , (1996).
[4] J.L. Batoz and G. Dhatt , *Modélisation des structures par éléments finis*, (Hermes,Paris, 1992).
[5] Z. Wang and A.N. Norris , *Waves in cylindrical shells with circonferential submenbers: A matrix approach*, Journal of Sound and Vibration, vol. **181**, 457-484, (1995).
[6] C. R. Fuller and F. J. Fahy , *Characteristics of wave propagation and energy distributions in cylindrical elastic shells filled with fluid*,Journal of Sound and Vibration, **81**, 501-518, (1982).
[7] R.S. Langley, *Wave evolution, reflection, and transmission along inhomogeneous waveguides*, Journal of Sound and Vibration, **227**, 131-158,(1999).
[8] V.A. Yakubovich and V.M. Starzhinskii, *Linear differential equations with periodic coefficients*,(Halsted Press, New York).
[9] S. Finnveden , *Spectral finite element analysis of the vibration of straight fluid-filled pipes with flanges* , Journal of Sound and Vibration, **199**, 225-154, (1997).
[10] Junger and D. Feit *Sound, Structures, and Their Interaction*, (second edition, Cambridge, Massachusetts, M.I.T. Press).
[11] Schaum
[12] B.R. Mace, *The statistics of power flow between two continuous one-dimensional subsystems*, Journal of Sound and Vibration,**154** , 321-341, (1992).
[13] G.V. Borgiotti, *Power flow analysis of surface waves on a cylindrical elastic shell in an acoustic fluide.*, J. Acoust. Soc. Amer., **95**, 244-255, (1994).
[14] Y. Yong and . Y.K. Lin, *Dynamic response analysis of truss-type structural networks: A wave propagation approach*, Journal of Sound and Vibration, **156**, 27-45, (1992).
[15] D.W. Miller and A. Von Flotow, *A travelling wave approach to power flow in structural networks*, Journal of Sound and Vibration, **128**, 145-162, (1989).

8. Annexe.

$$\underline{\underline{J_a}}^{(c)} = \begin{pmatrix} 0 & -\underline{\underline{I}}_{n+3} \\ \underline{\underline{I}}_{n+3} & 0 \end{pmatrix}, \quad \underline{\underline{B}} = 2\sqrt{\pi}\, a \begin{pmatrix} 0 & \dots & 0 \\ 1 & \dots & 1 \\ 0 & \dots & 0 \end{pmatrix}, \quad \underline{\underline{M}}^{(s)} = \frac{1}{2\pi a} \begin{pmatrix} 1/C & 0 & 0 \\ 0 & 0 & 0 \\ 0 & 0 & 1/D \end{pmatrix}$$

$$\underline{\underline{K}}^{(s)} = 2\pi a \begin{pmatrix} \rho h\omega^2 & 0 & 0 \\ 0 & \frac{h(-E+\rho\omega^2 a^2)}{a^2} & 0 \\ 0 & 0 & 0 \end{pmatrix}, \quad \underline{\underline{Q}}^{(s)} = \begin{pmatrix} 0 & 0 & 0 \\ -\frac{\nu}{a} & 0 & 0 \\ 0 & 1 & 0 \end{pmatrix}$$